PCCP

Accepted Manuscript

ROYAL SOCIETY OF CHEMISTRY

www.rsc.org/pccp

Unravelling the hydrogen absorption process in Pd overlayers on a Au(111) surface

Paola M. Quaino,*,† Renat Nazmutdinov,‡ Leonardo F. Peiretti,† and Elizabeth Santos¶,§

†*PRELINE, Fac. de Ing. Química, Universidad Nacional del Litoral, 3000 Santa Fe, Argentina*

‡*Kazan National Research Technological University, 420015 Kazan, Russian Federation*

¶*Institute of Theoretical Chemistry, Ulm University, D-89069 Ulm, Germany*

§*Facultad de Matemáticas, Astronomía y Física, IFEG-CONICET, UNC, Argentina*

E-mail: pquaino@fiq.unl.edu.ar

Abstract

The hydrogen absorption into overlayers of Pd deposited on Au(111) has been investigated by density functional theory (DFT). Hydrogen concentrations, absorption environments, geometrical and electronic effects have been analyzed, seeking for a better understanding of the general principles governing the process and the effect of foreign supports. The results show that the absorption is more favored than in pure Pd leading to lower absorption energies and less repulsive interactions due to the surface expansion induced by the gold larger lattice constant. Our findings also suggest that the hydrogen absorption process is more favorable for lower number of Pd overlayers. This situation changes gradually until the substrate influence is no longer detected and the pure palladium nature appears. An entangled combination of repulsive forces, strain effect, structural ordering and chemical affinity has been found. The kinectis

of hydrogen absorption has been studied as well. Two cases were explored: 1) the absorption of an adsorbed hydrogen atom and 2) the bond-breaking and penetration of a H_2 molecule.

1. Introduction

In surface science the interaction of hydrogen with metal surfaces was always of pivotal interest, not only from the viewpoint of fundamental theory, but also due to its great technological impact on many processes such as energy storage and conversion,[1,2] hydrogenation reactions,[3,4] bulk absorption (embrittlement),[5] among others.

In electrochemistry, the hydrogen reaction is of great importance due to its participation in the fuel cell technology. It takes place through the well known Volmer-Heyrovsky-Tafel mechanism, where an adsorbed hydrogen atom acts as a reaction intermediate on an active site on the metal electrode.[6–8] To understand the behavior of the intermediate and the role of the electrocatalyst (substrate), the adsorption and absorption of hydrogen and their interplay are of major interest.

For many decades, various mechanisms have been proposed for the adsorption-absorption processes on Pd. A one-step route has been initially proposed by Bagotskaya[9] and Frumkin,[10] where hydrogen enters directly into the metal without going through any intermediate adsorbed state. A two-steps route has been proposed by Bockris et al,[11] where hydrogen absorption occurs indirectly: first the adsorption on the metal surface takes place, accompanied by chemical absorption into the subsurface metal layer. Recently, Sakong et al[12] have also suggested a concerted mechanism, where the subsurface penetration of a hydrogen atom involves another hydrogen atom at an adjacent bridge site in a concerted manner.

Additionally, in an electrochemical environment simultaneously with the absorption, hydrogen evolution reaction takes place, involving one of two possible further steps: the chemical or electrochemical recombination (Tafel and Heyrovsky mechanisms, respectively). Similar to metal deposition, hydrogen adsorption can occur at both, higher and lower potentials,

than the predicted thermodynamical values given a weakly and a strongly adsorbed species, overpotential (OPD) and underpotential (UPD) deposition, respectively.[13]

Pd hydrides show a quite complicated phase diagram with two main forms, α- and β-PdH_x.[14] The former appears at low, while the latter at high contents of hydrogen. It has been shown that hydrogen evolution occurs only after the β-phase formation.[14] Although the presence of both, H_{ad} (adsorbed hydrogen) or H_{ab} (absorbed hydrogen) affects the nature of the substrate, most of the known work is focused on hydrogen adsorption on metals. An excellent review on this topic can be found in Christmann's book.[15]

Practically all pure metals and alloys have been tested as possible electrocatalysts for the hydrogen reaction to find something cheaper and better than Pt. Nowadays attention is attracted on nanostructured electrodes, like metals covered by monolayers, or clusters of another metal or core-shell particles. In this context, a combination of Pd and Au seems to be a promising catalyst and a wide variety of combinations was deeply investigated at both, theoretical and experimentally. For instance, hydrogen adsorption on overlayers of Pd on gold surfaces was studied by Roudgar et al.[16,17] and Gross.[18] The stability of Pd monomers, dimers or trimers in the surface or subsurface layers of Au(111) and the influence on the hydrogen adsorption were investigated by Venkatachalam et al.[19] In addition, experimental findings related to the hydrogen evolution/oxidation on Pd-Au systems have been supported by theoretical studies such as those in the group of Nørskov[20–22] and in our own group.[23–27] We have systematically investigated the effect of the substrates on the electronic properties of Pd-nanostructures. We have also focused on the hydrogen evolution and oxidation at Pd-Au nanostructures by means of both experiment and theory.[24] In contrast, there is a lack of knowledge about the hydrogen absorption on bimetallic surfaces and most of the work is mainly centered on pure transition metals, such as Pd,[28,29] Ni,[30] Fe,[31] Ru,[32] Rh, etc. and their different facets.[33,34] As the bulk palladium actively absorbs hydrogen, it is interesting to explore some features of this process occurring in layers of Pd adsorbed on other metal substrates. In this sense, different hydrogen related processes (i.e., adsorption,

absorption, diffusion, and desorption) occuring on Pd/Au(111) surfaces have been studied by means of temperature-programmed desorption (TPD) under ultra-high vacuum conditions.[35] The results reveal PdAu bimetallic surfaces weakly bind H adatoms while H absorption was observed when hydrogen was exposed at higher surface temperatures. The near-surface H was relatively unstable and desorbed at a lower temperature than adsorbed H. Oruga et al.[36] investigated the hydrogen interaction with a $Pd_{70}Au_{30}$ alloy by thermal desorption spectroscopy (TDS) and nuclear reaction analysis (NRA). The authors reported hydrogen accumulation in the near-surface region and absorption in the bulk of the alloy.

In a previous work, we have investigated the electrocatalytic properties of multilayers of Pd epitaxially deposited on Au(111).[37] We have focused on the kinetics of the electrochemical step for hydrogen adsorption (Volmer reaction) and determined the energy of activation by a combination of density functional theory calculations and our own theory of electrocatalysis, which allows to take into account the electrochemical environment explicitly. For two layers of Pd on Au(111) containing absorbed hydrogen in the subsurface, the adsorption free energy was found to be less negative and the barrier lower than pure Pd(111). This was in agreement with experimental data which showed a higher activity for hydrogen oxidation with hydride Pd systems. In another study, we have analyzed the Volmer step and the hydrogen absorption for a system containing a Pd layer underneath the Au(111) surface.[38] To the best of our knowledge, this is the only theoretical study of H absorption in overlayers of Pd on a gold substrate.

Herein, we focus on the absorption of H into pure Pd and overlayers of Pd deposited on Au(111) to gain a deeper insight into the general principles governing the absorption process and the effect of foreign supports in the absorption phenomena. Additionally we have investigated the penetration rate due to the possible existence of quantum tunneling.

This paper is organized as follows. Some pertinent details on model calculations are reported in the next Section. Then, we present the results of DFT calculations for the interaction of the H atom with Pd(111) and Pd_n/Au(111); different hydrogen concentrations,

absorption environments, geometrical and electronic effects are estimated and analyzed. The rate constants describing the absorption of H atoms from an adsorbed state are calculated as well. Concluding remarks are reported in the last Section.

2. Theory

DFT Calculations and Modeling

Periodic DFT calculations were performed using DACAPO code.[39] A plane-wave basis set was used to expand the electronic wave functions, and the inner electrons were represented by ultrasoft pseudopotentials,[40] which allows the use of a low-energy cutoff for the plane-wave basis set. Special care was taken for the parametrization of the energy cutoff and the k-points sampling of the Brillouin zone based on the Monkhorst-Pack grid.[41] Both parameters were increased systematically until the change in the absolute energy was less than 10 meV. An energy cutoff of 450 eV and a grid of $8 \times 8 \times 1$ satisfied the energy accuracy. The electron-electron exchange and correlation interactions were treated with the generalized gradient approximation in the version of Perdew et al. (PBE).[42] Application of this functional on bulk Au and Pd results in theoretical lattice parameters of a_0^{Pd}=3.99 Å and a_0^{Au}=4.18 Å. Within the typical margins of error, both constants agree with the experimental data (a_0^{Pd}=3.89 Å and a_0^{Au}=4.08 Å) reported in the literature.[43] To evaluate the influence of the exchange-correlation functional employed, test calculations were performed using PW91 version.[44] Resulting modifications in energetics and structure were negligible.

In all the calculations spin polarization was considered but no effect was found. Dipole correction was used to avoid slab-slab interactions.[45]

To study the hydrogen absorption process several systems were considered: a pure metal surface -Pd(111)- and overlayers of Pd_n (n=1,2,3,4) on Au(111). The pure Pd(111) surface was modelled by a (2×2) supercell with 5 metal layers. For the alloy, a (2×2) supercell with 4 substrate-layers -Au(111)- and n (n=1,2,3,4) adatom-overlayer(s) were used.

In all the calculations a vacuum corresponding to 12 Å was used. For all the systems, the three bottom layers were fixed at the next-neighbor distance corresponding to bulk and all the other layers were allowed to fully relax. The convergence criterion was achieved when the total forces were less than 0.02 eV/Å.

First, the hydrogen atoms were positioned in two possible interstitial absorption sites between the metal layers: tetrahedral and octahedral environments according to the hydrogen coordination (see Fig.1) and allowed to relax in the xyz coordinates in order to find their equilibrium positions. The effect of the hydrogen concentration[1] was investigated for pure Pd and for n=2,3 overlayers of palladium ([H]=0.25, 0.5, 0.75, 1.0). Finally, we have also calculated the absorption energies as a function of the number of palladium overlayers (n=1,2,3,4) for a full concentration of hydrogen for both environments, tetrahedral and octahedral.

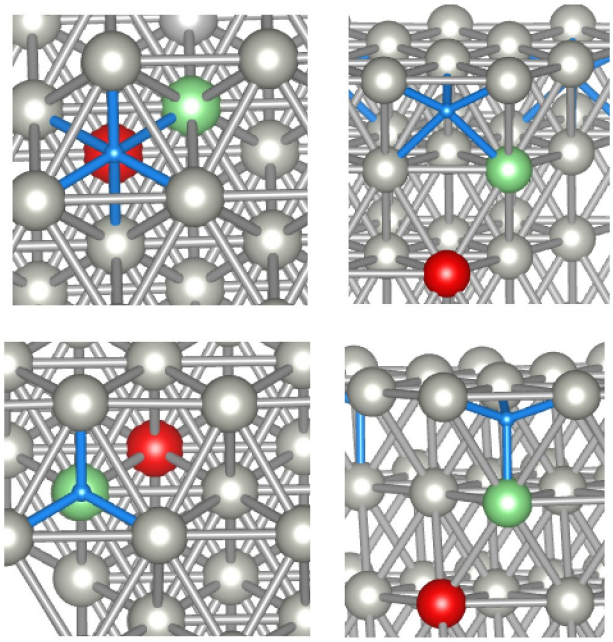

Figure 1: Hydrogen absorption in Pd(111). Top row: Octahedral site. Coordination: 6 (top and side views). Bottom row: Tetrahedral site. Coordination: 4 (top and side views). Red ball corresponds to the third metal layer, green ball corresponds to the second metal layer. Light blue balls correspond to hydrogen atoms.

[1]The hydrogen concentration [H] is defined as the number of hydrogen atoms per primitive surface unit cell divided by the total number of specific sites, tetrahedral or octahedral.

The penetration of hydrogen in the presence of pre-adsorbed hydrogen on the Pd_2/Au(111) surface was evaluated with the nudged elastic-band (NEB) method[46,47] to find the minimum energy paths and the corresponding activation barriers using seven images of the system along the transition path. Within this method the initial and final states are known and a chain of beads is connected by harmonic springs (k=0.1 $eV/\mathring{A}^2$) between reactant and product states. The general parameters used for the NEB calculations are the same as for the previous DFT calculations described above.

We also performed model calculations to investigate the absorption rate of a hydrogen atom. The friction coefficient[2] η which governs the motion of a H atom in the adsorption well can be estimated as follows (see pag. 59 in ref.[48])

$$\eta \approx \frac{\varepsilon_F m_e}{\hbar m_p} \tag{1}$$

ε_F is the Fermi level of a metal, m_e and m_p are the electron and proton mass, respectively.

As a typical value of ε_F lies in the interval 5 – 10 eV, the friction amounts to $\sim 10^{13}$ s^{-1} which is comparable with the vibrational frequency values of adsorbed H atoms, $\nu_\pm$ (see Table 4). We can employ, therefore[48] the transition state theory to describe the absorption rate constant (k_{ab}):

$$k_{ab} = \nu_\pm \exp(-\Delta E_a / k_B T) \tag{2}$$

where the activation energy is ($\Delta E_a = E_{max} - \varepsilon_0$), E_{max} is the maximum energy value of potential energy surface and ε_0 is the zero vibrational energy at 300 K.

The frequency $\nu_\pm$ was calculated in harmonic approximation. If quantum tunneling is addressed, eq. 2 should be re-written:

[2]The physical meaning of the friction coefficient is that a hydrogen atom in a potential well (being a light particle) "feels" the electron bath in a metal more than the phonon bath generated by the slow modes of atomic nuclei. Eq. 1 provides a resonable estimate of this quantity, because it originally describes the relaxation rate of the H atom at its transition from the vibrational energy level n to $n-1$.

$$k^*_{ab} = \nu \sum_i p_i \exp(-\Delta E^{(i)}_a / k_B T) \quad (3)$$

where p_i is the tunneling probability from the i^{th} vibrational energy level of initial well to the nearest level of the final well; as shown in eq. 4. $\Delta E^{(i)}_a$ is defined as before, ($\Delta E^{(i)}_a = \varepsilon_i - \varepsilon_0$), being ε_i the energy of the i^{th} vibrational level of potential energy surface and ε_0 the zero vibrational energy at 300 K.

In the quasi-classical approximation we have,

$$p_i = \exp \frac{-2}{\hbar} \int_{xL}^{xR} \sqrt{2m(U(x) - \varepsilon_i)} dx \quad (4)$$

where $U(x)$ is a potential energy surface describing the energy barrier region; x_R and x_L are the right and left turning points, respectively.

To find the proton vibrational energy levels in two-dimentional potentials of an arbitrary form, we employed the original technique described previously in Ref.[49] In this case, the Schrödinger equation of second order is reduced to a differential equation of first order which is integrated numerically. The accuracy of this method is higher than the frequently used Numerov's scheme.

Pd(111) and Pd_3/Au(111), as well as a sandwich-like system – Au/Pd/Au(111) – taken from literature[38] have been investigated.

3. Energetics, Structure and Electronic Properties

Hydrogen adsorption on Pd and Pd-Au systems are well-documented topics from an experimental and a theoretical point of view.[16–18,21,23,24,50–57] Specifically, the study of hydrogen adsorption on a different number of palladium overlayers on Au surfaces was reported by Roudgar et al.[16] However, the lack of attention to the absorption phenomena on these systems is a tempting motivation to seek a deeper understanding of such process.

In this context, we have systematically investigated the hydrogen absorption in both systems, Pd(111) and Pd_n/Au(111). To begin with, a pure Pd(111) – surface has been considered as a reference and studied for two different absorption environments – octahedral and tetrahedral (Table 1). The effect of the hydrogen concentration ($[H]$) was also evaluated. The absorption energy (E_{ab}) has been calculated by the following expression:

$$E_{ab} = (E_{H_m - Pd(111)} - E_{Pd(111)})/m - 1/2E_{H_2} \quad (5)$$

Here, the first term corresponds to the energy of the relaxed system H_m−Pd(111) with the hydrogen at the absorption equilibrium position in the subsurface, being m the number of hydrogen atoms; the second term corresponds to the energy of the relaxed Pd(111) surface without hydrogen; the third term is half the energy of a hydrogen molecule in vacuum. Calculated energy values plus structural parameters such as % of expansion [3] and hydrogen perpendicular distance bewteen the first two layers are shown in Table 1.

Our results indicate that the presence of hydrogen underneath the surface originates geometrical perturbations in the upper metal layer, and the absorption was found to be stable after optimization for all the hydrogen concentrations investigated. These results are in good agreement with previously reported data.[58,59] The absorbate-induced configurational changes are sensitive to the hydrogen concentration and to the absorption site as well. Such *wave-like configuration* found in the first layer was detected in both environments, but much more noticeably in the tetrahedral one (Fig. 2). In the octahedral site, the modifications in the surface due to the presence of hydrogen are subtler and the material seems to remain *geometrically* comparable to pure palladium. Due to the features of the tetrahedral site, the repulsion is stronger leading to higher expansion. This findings are in agreement with the expansion parameter (%Δ), which increases with the amount of hydrogen in both cases (see Table 1).

[3]The expansion (%Δ) has been calculated between the first and second layers after H absorption, and relative to the same interlayer distance previous the absorption.

Table 1: Absorption energy (eV/atom) in the case of pure Pd(111) as a function of the hydrogen concentration $[H]$ for the octahedral and tetrahedral sites. The average of the hydrogen perpendicular distance (Å) and the % of expansion after hydrogen absorption respect to the pure Pd surface are also informed.

	Octahedral Site			Tetrahedral Site		
$[H]$	E_{ab}	$\overline{z}_H^{\perp}$	$\%\Delta$	E_{ab}	$\overline{z}_H^{\perp}$	$\%\Delta$
0.25	-0.238	-0.835	1.7	-0.204	-0.558	2.5
0.50	-0.233	-0.855	2.7	-0.213	-0.653	5.9
0.75	-0.224	-0.910	5.1	-0.223	-0.736	9.7
1.00	-0.209	-0.955	6.4	-0.230	-0.821	13.5

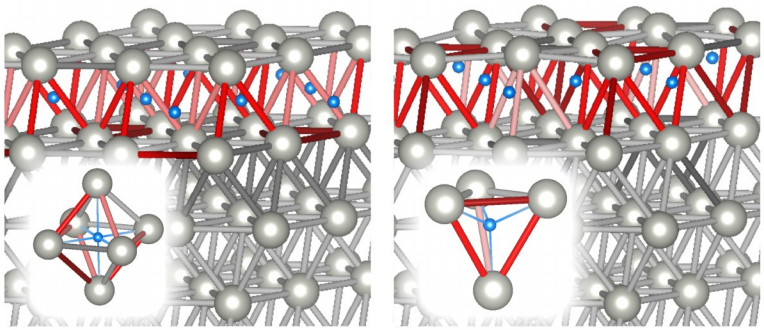

Figure 2: Side view of hydrogen absorption (light blue balls) in Pd(111) (grey balls). $[H] = 0.75$. Sites: octahedral (left), tetrahedral (right). Bond distance variation is identified by a gradient of colors: light red is the longest Pd-bond distance, dark grey is the smallest one. The inset figures illustrate the H coordination in each case.

The energetic analysis from Table 1 let us to conclude that:

i) the octahedral position is the most favorable environment leading to lower absorption energies when the hydrogen concentration decreases.

ii) the tetrahedral position is the most favorable environment leading to lower absorption energies when the hydrogen concentration increases.

These opposite dependencies are very interesting. They can be attributed to less repulsive interactions and less structural expansion in the octahedral site; while in the tetrahedral one important surface relaxations prevail over repulsive forces, leading to higher order structure as the hydrogen concentration increases.

To evaluate the influence of the substrate and the behavior of hydrogen, we have investi-

gated the absorption phenomena in Pd overlayers on Au(111). The investigations have been carried out for different number of Pd layers and hydrogen concentrations. The absorption has been restricted and hence analysed between the first and second metal layers. We refer to these systems as $Pd_n/Au(111)$, where n=1,2,3,4 corresponds to the number of palladium layers on a gold surface. The absorption energies have been computed by

$$E_{ab} = (E_{H_m - Pd_n/Au(111)} - E_{Pd_n/Au(111)})/m - 1/2E_{H_2} \quad (6)$$

where the first term corresponds to the energy of the relaxed system $H_m{-}Pd_n/Au(111)$ with the hydrogen at the absorption equilibrium position under the first Pd layer of the $Pd_n/Au(111)$, being m the number of hydrogen atoms and n the number of Pd layers; the second term corresponds to the energy of the relaxed system $Pd_n/Au(111)$ without hydrogen; the third term is half the energy of a hydrogen molecule in vacuum.

The first investigated system is Pd_1/Au. We found that the Pd-Au interface is an exceptional case. As expected, after structure relaxations, no hydrogen was found underneath the surface [4]. Calculations carried out for both sites, tetrahedral and octahedral, showed that no absorption takes place. The optimized structures exhibited only adsorbed hydrogen. According to experimental information reported by Baldauf et al.,[60] no hydrogen absorption was detected for one palladium monolayer on a gold surface. Additionally, it is well known that hydrogen adsorption energy is endothermic on bare gold surfaces.[24,61] Hence, we conclude that gold repel hydrogen atoms and the absorption phenomena is not favored for one monolayer of Pd on Au. Furthermore, it can be conjectured that if the surface behaves like a valve and hydrogen start to diffuse into the bulk after saturation, adding hydrogen to a full ML of H on $Pd_1/Au(111)$ will not induce the penetration of the pre-adsorbed H atoms due to the high activation barrier at the Pd–Au interface.

This situation changes when more overlayers of palladium are deposited on gold. The

[4] According to our technical methodology, the hydrogen atom was located at the octahedral or tetrahedral site before optimization. This configuration has been taken as an initial state.

absorption is favorable and hydrogens are localized between the first and second layer of Pd. The absorption energy for the tetrahedral and octahedral sites are given in Table 2.

The absorption underneath the surface is only favorable at high concentration of hydrogen; for lower [H] the adsorption was found favorable. In the case of 2 Pd overlayers, the process is exothermic for [H]=0.75 and 1.00. Nevertheless, in the case of 3 Pd overlayers no absorption takes place in the octahedral site for [H]=0.75 (see Table 2). An analysis of the energetics indicates that the absorption in the tetrahedral site is more favorable than in the octahedral one (see Table 2).

Absorption in the octahedral environment shows a similar behavior that for pure Pd. The absorption energy rises with the hydrogen atom concentration due to an increase of the repulsion. In this case, the larger lattice constant of Au induces a relative expansion of the Pd layers, allowing for a better localization of hydrogen atoms at the interstitial sites of Pd_n/Au(111) and leading, in consequence, to less repulsive interactions and to lower absorption energies (more favorable) in comparison to pure Pd. The opposite trend was found for pure Pd at the tetrahedral environment. Here, the absorption energies are lower when the concentration increases, leading to larger stability. This fact can be attributed to the smaller lattice constant of palladium, which leads to a more compressed surface with smaller interstitial sites. Indeed, the structure expands vertically to diminish the interactions, conducting to a higher order structure when the amount of hydrogen rises.

Table 2: Hydrogen absorption energies (eV/atom) for octahedral and tetrahedral sites in the case of Pd_n/Au(111) n=2,3. Different hydrogen concentrations underneath the first two atoms layers were tested. No absorption has been found after structural optimization for low hydrogen concentrations (0.25 and 0.5).

	Pd_2/Au(111)				Pd_3/Au(111)			
$[H]$	octahedral		tetrahedral		octahedral		tetrahedral	
	E_{ab}	%Δ	E_{ab}	%Δ	E_{ab}	%Δ	E_{ab}	%Δ
0.75	-0.446	4.3	-0.475	6.0	–	–	-0.458	6.3
1.00	-0.417	5.7	-0.436	10.3	-0.396	6.3	-0.435	10.5

For completeness, the influence of the number of palladium layers on the absorption process was compared for a full monolayer of absorbed hydrogen in Pd_n/Au (n=2,3,4). The energetic information is summarized in Table 3. The absorption energy for palladium was also included to be considered as reference.

The results indicate that for the octahedral environment, the energy values become higher – but lower than pure Pd – as the number of palladium layers increases. Interestingly, for the tetrahedral sites, the minimun in absorption energies appears for two ($E_{ab} = -0.436$ eV/atom) and three ($E_{ab} = -0.435$ eV/atom) palladium layers, although for four layers the process is still favorable ($E_{ab} = -0.407$ eV/atom). These results are in agreement with the experiments reported by Baldauf et al.:[60] These authors suggest that no appreciable amount of hydrogen was detected at the first two palladium layers, however significant amount of hydrogen appeared at the third.

Table 3: Hydrogen absorption energies for octahedral and tetrahedral sites in the case of Pd_n/Au(111) n=2,3,4 and pure Pd(111) for a full monolayer of hydrogen underneath the first two atoms layers. For comparison, the adsorption energy (eV/atom) for the fcc-hollow site at $\theta = 0.25$ is shown in parentheses.

Systems	E_{ab}(octa) [eV/atom]	E_{ab} (tetra) [eV/atom]
Pd_2/Au(111)	-0.417 (-0.69)	-0.436
Pd_3/Au(111)	-0.396 (-0.66)	-0.435
Pd_4/Au(111)	-0.372 (-0.64)	-0.407
Pd(111)	-0.209 (-0.58)	-0.230

Our data indicate that in both environments the absorption phenomena is more favored than in pure Pd, leading to lower absorption energies and less repulsive interactions due to the surface expansion induced by the gold larger lattice constant. These theoretical findings also suggest that the hydrogen absorption process at the subsurface sites is more favorable for lower number of Pd overlayers. This situation changes gradually until the substrate influence is no longer detected and the pure palladium nature is found. As can be seen from Table 3, the adsorption energy values lie deeper (ca 0.2 eV) as compared with those found

for the absorbed positions. Therefore, the latter can be considered for these systems as a metastable state.

We have also analysed the changes on the electronic properties of Pd overlayers. A comparison of the d bands for the systems – $Pd_n/Au(111)$, n=1,2,3,4 – is shown in Fig. 3. The band structure for the bare Pd(111) are also included for comparison. The DOS of the d bands changes markedly for $Pd_1/Au(111)$. The band appears shifted to more positive energies (Fig. 3: red line) compared to pure Pd surface (Fig. 3: black line, grey shaded area). It becomes thinner, indicating a stronger localization of the electrons. The lattice constants misfiting induces the well-known strain in the overlayer, which also causes a change in the electronic properties. However, the modifications in the electronic structure are also a consequence of the chemical interplay due to direct contact with the gold substrate. Therefore, it is expected that the d band profiles for the surface of $Pd_n/Au(111)$ tend to the d band of palladium with increasing n (Fig. 3), due to the lesser substrate influence. The upshift of the d bands to more positive energies and the narrower profiles are generally associated with a higher reactivity and follows the expected trend: $Pd_2/Au(111) > Pd_3/Au(111) > Pd_4/Au(111) > ... > Pd_n/Au(111) \approx Pd(111)$; in accordance with the trend in the absorption energy shown in Table 3.

A clarification is needed before proceeding: some DFT code take advantage of periodicity to handle the electronic structure problem for infinite solids in 3D simulation cells. In the case of surfaces, periodic boundary conditions are only applied in two dimensions, but the idea of a 3D simulation cell can be employed to simulate a surface by introducing a vacuum region in the remaining dimension, e.g. z-direction. Thus, the simulation cell is divided in two domains: a solid region (known as a slab) and a vacuum region. Due to the 2D periodicity, when a surface relaxation is performed in all the coordinates (xyz) only displacements in the unfixed atom layers are detected, which move inward or outward along the surface normal (z-direction). Alterations in the geometry involving lateral displacements (xy-directions) can not be mimic by periodic DFT. Taking into account the limitations of

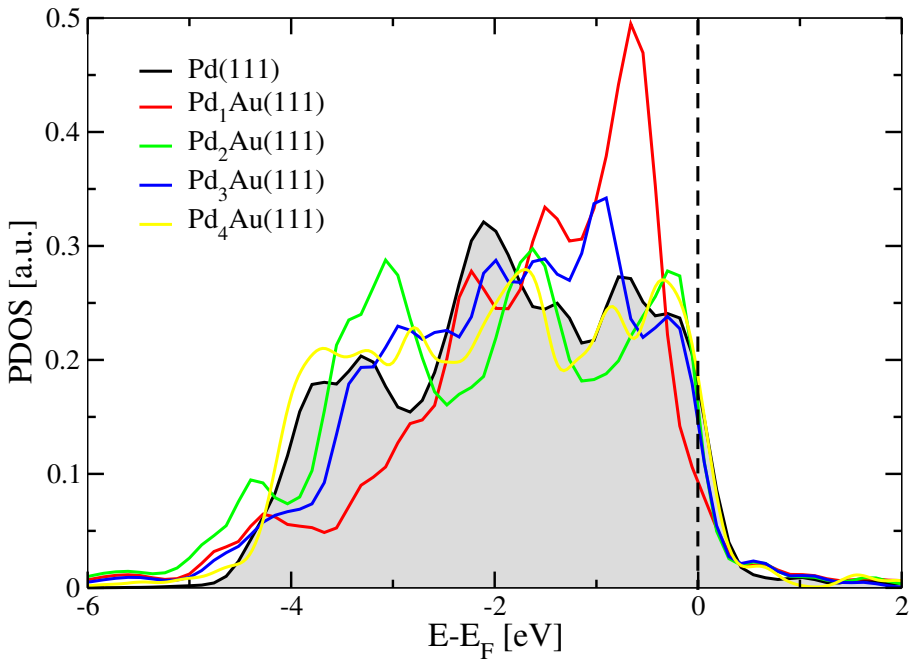

Figure 3: Density of states projected on the d bands for systems under study: black line – grey shaded area: Pd(111), red line: Pd_1/Au(111), green line: Pd_2/Au(111), blue line: Pd_3/Au(111), yellow line: Pd_4/Au(111). The vertical line indicates the position of the Fermi level.

the model outlined above, a simple relaxation procedure of Pd_n/Au (where all the Pd layers plus the first Au layer were allowed to optimize) will exhibit only geometrical modifications – expansions or compresions – in the direction of the surface normal (for completeness see Fig. 4). This restriction prohibits us to detect the lateral structural changes as the number of Pd multilayers increases. Hence, the lateral expansion due to the lattice constant mismatch will remain fixed. With this in mind, we have found that the lattice constant of Pd expanded 4.8% when is located over the Au surface. For obvious reasons, those changes should gradually tend to the properties of bulk Pd as the number of Pd layers rises. With this limitation in mind, we can extrapolate our results trying to represent them by the following model (Fig. 5):

Interface Pd–Au: formed by the gold surface layer in contact to the first palladium metal layer. The substrate induces geometrical expansion plus a direct chemical influcence on the Pd layer. Strong changes in the Pd electronic structure are identified (see Fig. 3).

These results are in agreement with previous studies.[16,23] Hydrogen absorption is forbbiden for n=1. Fig. 5: right side, dark orange color.

Modified Pd: formed by Pd overlayers (n=2, 3, 4,etc.). Chemical and structural factors decrease as the number of Pd layers rises. Therefore in the limit (thicker Pd films), bulk palladium behavior appears. Our energetic values suggest a progressive change as a function of Pd thickness (Table 3). Fig. 5: right side, dark grey color.

Bulk Pd: No chemical nor structural effects of the substrate are detected. Fig. 5: right side, grey gradient.

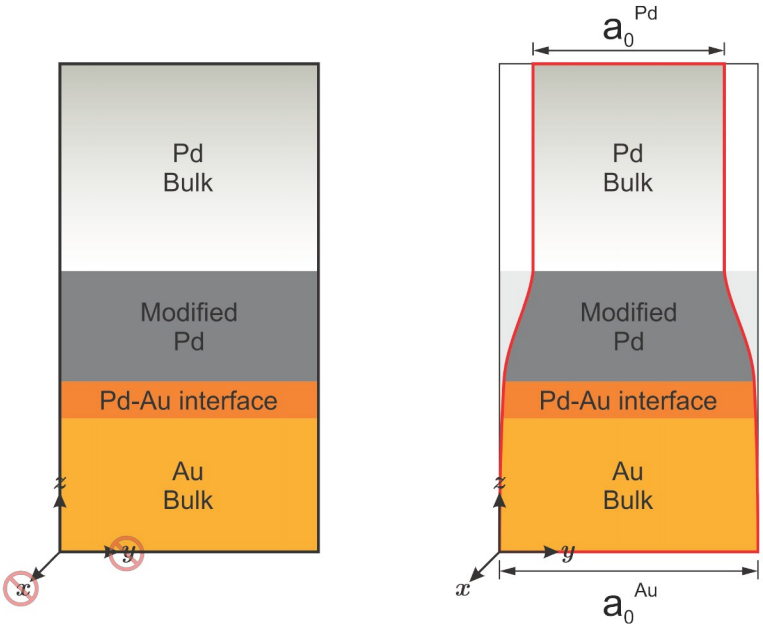

Figure 4: Model of Pd multilayers on Au(111) surface. The yellow area corresponds to Au surface and the grey area represents Pd layers. The gradient of grey color indicates differences between the layers of Pd as they move away from the gold surface; the darker the grey, the closer to Au(111) surface. The Pd-Au interface is illustrated in orange. Left side: DFT modeling. Right side: expected behavior of a real system.

4. Artificial Systems - Theoretical Experiments

The changes on the reactivity previously depicted are too complex to be explained only by a modification of geometrical arrangements. Specific chemical interactions between the

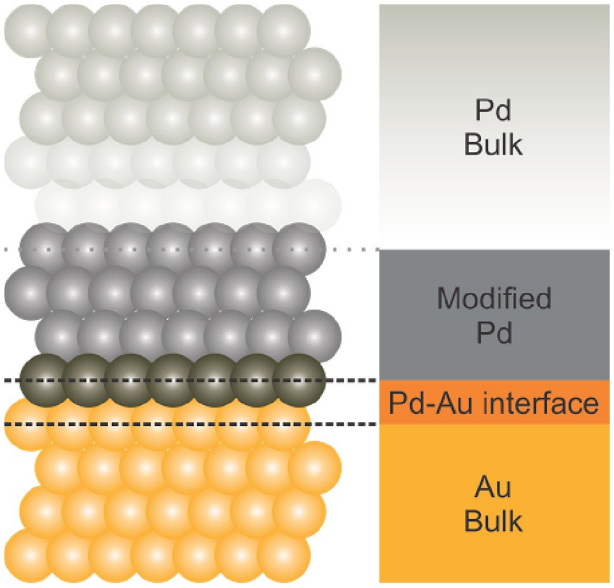

Figure 5: Model for hydrogen absorption in Pd overlayers on Au. Left side: yellow balls: Au atoms, grey balls: Pd atoms. The gradient of grey color indicates differences between the layers of Pd as they move away from the gold surface; the darker the grey, the closer to Au(111) surface. Right side: each zone is indicated by colors matching the structure on the left side.

substrate and the foreign metal ad-layers play an important role as discussed by us in a previous work.[23]

Seeking for a better understanding of the influence of the strain and chemical effects on the absorption process, theoretical experiments have been performed to decouple these two effects from each other and to investigate their effects separatedly. Ergo, the question now is: what happens when Au behaves like Pd and the other way around?

In this sense, virtual systems have been modeled according to the procedure discussed in the literature:[23,62] We have replaced the value of the lattice constant of Pd by that corresponding to Au(111) in the Pd(111) system, and *vice versa*. Then we calculated the density of states and the absorption energy as a function of $[H]$ with this fixed value, not allowing the system to relax. Obviously, these are not real systems but their energetic and electronic behaviors allow us to distinguish between the strain effect and the role played by the chemical interactions between the foreign metal and the substrate. Fig. 6 shows the comparison of the electronic properties for the artificial and real systems.

Due to the lattice constant mismatch between Au and Pd, changes in the electronic states distribution and shapes are expected in the virtual systems. Fig 6 (top panel) shows the d and sp bands of a Pd surface with the geometrical structure of gold (a_0^{Au}). In comparison to bulk Pd, the former exhibits thinner d band structure shifted to higher energies, showing stronger electron localization. The same trend is also found in the sp bands. These changes in the electronic properties enhance the structure reactivity. As a consequence, an improvement in the absorption energies has been detected for both sites when compared to Pd(111), as can be observed in Fig 7. Furthermore, the calculated energies of the artificial palladium are even better than those obtained for Pd_n/Au(111) n=2, 3, 4.

On the other hand, the lattice constant of Au have been replaced by the one correspoding to Pd, and the calculated density of states projected on the d and sp bands of a Au surface with the geometrical structure of palladium (a_0^{Pd}) are shown in Fig. 6, botton panel. The opposite behavior has been found: the bands are thicker and shifted to lower energies in comparison to bulk Au. The effect of the lattice constant can be clearly observed. In this case, a_0^{Pd} is smaller than a_0^{Au} and obviously, the number of gold electrons remains constant. Thus, if the lattice constant decreases, the delocalization of the orbitals increases, producing the extension of the d band into lower energies. Absorption energies have been evaluated and showed endothermic values for all $[H]$.

The latter findings, in combination with the results presented in Table 2, let us conclude the existence of a tangled interplay between the strain, chemical and repulsive interactions. Chemical interactions induced by the gold substrate can be observed. For Pd(111) and Pd(111)-a_0^{Au}, absorption has been found for all $[H]$, while for Pd_n/Au(111) n=2, 3 the absorption has only been found for higher amount of hydrogen underneath the surface. This behavior can be understood as a blending of repulsive forces, strain effect, structural ordering and chemical affinity.

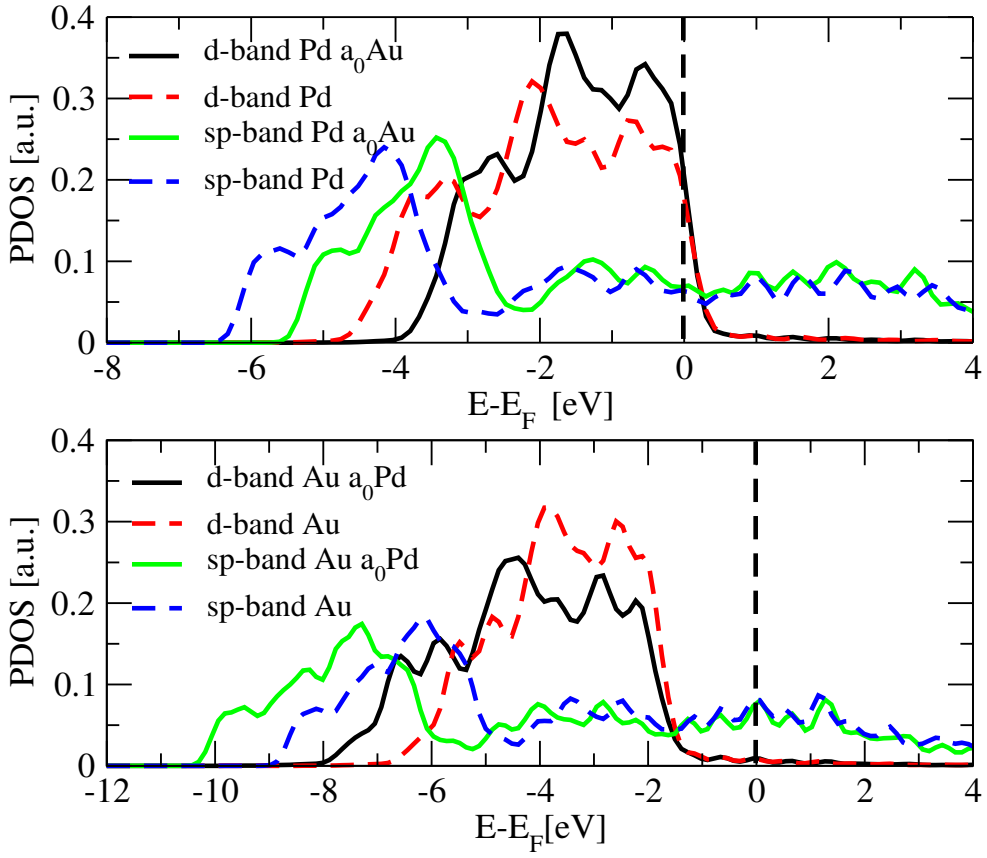

Figure 6: Projected Density of states: Upper panel, d bands: black line: Pd(111) with a_0^{Au} and red dashed line: Pd(111) and sp bands: green line: Pd(111) with a_0^{Au}, blue dashed line: Pd(111). Botton panel, d bands: black line: Au(111) with a_0^{Pd} and red dashed line: Au(111) and sp bands: green line: Au(111) with a_0^{Pd}, blue dashed line: Au(111). The vertical lines indicate the position of the Fermi level.

5. Kinetics and Reaction Paths for the Absorption of Hydrogen

Hydrogen absorption mechanisms have been deeply studied for Pd(111) and are well documented.[9–12,58] In electrochemistry, the hydrogen absorption is a complicated reaction due to the parallel ocurrence of other processes such as: hydrogen evolution and hydrogen adsorption (UPD and OPD hydrogen[13]). As described in Section 1, several mechanisms have been proposed for Pd(111): direct absorption,[9,10] indirect absorption[11,63] and a concerted mechanism[12] has been suggested as well.

To investigate the hydrogen penetration process in electrochemistry, we have considered two cases: as a first approximation, a fully hydrogen covered Pd_2/Au(111) surface, corresponding to the strongly adsorbed hydrogen or the well-known hydrogen deposited at underpotential (H_{UPD}, where the adsorption sets in at potentials above the hydrogen evolution); and as a second option, a H_2 molecule approaching to a Pd_2/Au(111) surface pre-covered with a submonolayer of hydrogen and its subsequent subsurface penetration.

a) Scenario A: Subsurface penetration of adsorbed hydrogen

Our results show that the subsurface penetration of a single hydrogen atom is hindered by a barrier of about $\approx$ 0.2 eV (Fig. 8, red line). At the final state, the hydrogen atom is located at the octahedral site underneath the first surface layer. For simplicity, the initial state has been taken as reference to recast the energy values, i.e. E^{ini}=0. A hydrogen atom moving through the first Pd layer has been identified as a transition state (see ESI for structure details). During the penetration, a subtle lateral expansion of the Pd atoms surrounding the hydrogen atom accompanies the main process.

b) Scenario B: Approach and subsurface penetration of a H_2 molecule

Beside the previous case, we have also considered a submonolayer of pre-adsorbed hydrogen (surface coverage θ_H= 0.75 ML) on the Pd_2/Au(111). This substrate has free surface sites, which allows us to investigate the behavior of a hydrogen molecule (for clarification, see the initial state configuration in the ESI: the hydrogen molecule has been identified in red to distinguish it from the pre-adsorbed hydrogen on the surface, in light blue). We positioned the molecule at 3.2 Å to minimize the interaction with the surface. The molecule axis was oriented perpendicular to the surface plane and centered to the hole site as shown in the ESI. As follows from our results, the higher barrier ($\approx$ 0.4 eV) originates from the molecule re-orientation almost parallel to the surface, with one hydrogen pointing to the hole and the other localized on a slightly shifted top site, as shown in image 2 in the ESI. Subsequently, as

the molecules approaches to the free fcc-hollow site, the H oriented closer to the hole starts a combined adsorption-absorption process, with a concomitant molecule bond breaking and the inmediate filling of the hollow site with the remaining hydrogen. The process is almost barrierless as can be observed in Fig. 8, black line; the third image shown in the ESI has been used to illustrate the evolution of the reaction. The final state is the most energetically favored configuration: a full ML of adsorbed hydrogen (θ_H=1.00) and a subsurface hydrogen ([H]=0.25) have been found as a product. This concerted mechanism is highly comparable to the one reported by Sakong et al.[12] for pure Pd(100).

Paul et al.[29] have calculated an energy barrier of about 0.8 eV for the absorption of hydrogen at an unrelaxed Pd(111). For an adlayer of hydrogen, the absorption of additional hydrogen into the surface site occurs via a concerted mechanism with an activation energy of 0.4 eV.[64] Other study shows a barrier of about 0.6 eV for the diffusion of H from the fcc-hollow site to the octahedral site at Pd(111) for 0.25 hydrogen ML.[65] If the direct absorption into the subsurface is considered, the reported energy barriers oscillate bewteen 0.9 eV for unrelaxed and 0.4 eV for relaxed surfaces.[66,67]

In the present paper we have found a barrier of about 0.3 eV for a low hydrogen coverage at a relaxed Pd(111) surface considering a direct absorption mechanism (not shown). The activation barriers found for the penetration process (Fig. 8) are considerably lower compared to the barriers reported for pure Pd(111) surfaces. Such important changes in the energetics can be attributed to the strain and chemical effects mentioned above, which facilitate the entry, adsorption and the bond-breaking process.

Absorption rate constants

Finally, the influence of quantum effects on the absorption rate has been addressed. The potential energy surfaces (PES) have been constructed for a hydrogen atom approaching to the fcc-hollow site on the surface and entering to the underneath octahedral site. No layers of adsorbed or absorbed H atoms were addressed. This energy surface may be attributed to

the very initial absorption stage. Although in this case the absorption state is less feasible as compared with adsorption position, we assume that the life time of a hydrogen atom in the metastable adsorbed state is enough to wait for further stabilization.

The double-well potentials constructed for Pd(111) and Pd_3/Au(111) do not favour the hydrogen tunneling, because they are significantly asymmetric and the energy minimum related to the absorbed state is very shallow. Therefore, for these systems quantum effects can take place only through zero vibrational level, ε_0, (eq. 3). We also considered an adsorbed deuterium atom (D) to investigate the kinetic isotope effect (KIE). Table 4 shows that the absorption of H (D) atom at the Pd_3/Au(111) surface proceeds faster as compared with Pd(111) which agrees with our findings described in Section 3. The KIE amounts to 2.6 – 2.7. It was already mentioned in Section 2 that for comparison we have performed similar calculations for a sandwich-like surface structure Au/Pd/Au(111) taken from literature.[38] Surprisingly, the tunneling effect decreases the rate constant for this system (Table 4). To conclude, classical overcoming the energy barrier was proven to be the most probable path for all the systems under study.

Table 4: Frequency factor ν, activation barrier ΔE_a, absorption rate k_{ab} and KIE calculated for Pd(111), Pd_3/Au(111) and Au/Pd/Au surfaces.

System	atom	ν [s^{-1}]	ΔE_a [eV]	k_{ab} [s^{-1}]	KIE
Pd(111)	H	1.87×10^{13}	0.323	4.60×10^{7}	2.6
	D	1.33×10^{13}	0.338	1.78×10^{7}	
Pd_3/Au(111)	H	5.20×10^{12}	0.148	1.40×10^{10}	2.7
	D	3.70×10^{12}	0.164	5.24×10^{9}	
Au/Pd/Au(111)[38]	H	2.40×10^{13}	0.304	1.25×10^{8} $(1.30 \times 10^{7})^a$	1.1
	D	1.70×10^{13}	0.298	1.14×10^{8} $(1.40 \times 10^{7})^a$	

[a]The values in parentheses correspond to the tunneling probability (see eq. 4).

6. Conclusions

In the present contribution we have investigated the absorption of hydrogen into overlayers of Pd on a Au(111) surface. We have analyzed in detail different factors that determine the thermodynamics and kinetics of the absorption process. Geometrical, chemical and electronic interactions between the Pd metal layers and the substrate play a complicated role, which is crucial to determine the subsurface penetration. Our results indicate that the absorption phenomena is more favored than in pure Pd, leading to lower absorption energies and less repulsive interactions due to the surface expansion induced by the gold larger lattice constant. These findings suggest that the hydrogen absorption at the subsurface sites is more favorable for less number of Pd overlayers. This behavior changes gradually until the substrate presence is not detected.

Concerning the kinetics, two cases have been studied: the subsurface penetration of an adsorbed hydrogen with an energy barrier of about 0.2 eV, and the approach and subsurface penetration of a H_2 molecule in the presence of adsorbed hydrogens. This mechanism shows a combined adsorption-absorption process, with a concomitant molecule bond breaking.

Finally, the influence of quantum effects on the absorption rate has been addressed indicating that classical overcoming the energy barrier was proven to be the most probable for all the systems under study.

There are two challenging effects which will be addressed in future model investigations. Firstly, we should mention the pressure influence on the adsorption-absorption interplay. Secondly, elucidating the role of vacancies (holes) in the surface metal layers would be of considerable interest.

Acknowledgement

This work is part of the research network financed by the Deutsche Forschungsgemeinschaft FOR1376. E.S. acknowledges PIP- CONICET-112-201001-00411 and PICT-2012-2324 P.Q.

thanks CAID 501 201101 00276 LI UNL and PICT-2014-1084 for support. A generous grant of computing time from the Baden-Württemberg grid is gratefully acknowledged. The authors also thank the support given by Santa Fe Science Technology and Innovation Agency (ASACTEI, grant 00010-18-2014) and CONICET for continuos support. R.N. thanks the Russian Foundation for Fundamental Research (project No 14-03-00935a)

References

(1) Sakintuna, B.; Lamari-Darkrim, F.; Hirscher, M. *Int. Journal of Hydrogen Energy* **2007**, *32*, 1121.

(2) Zhao, X.; Ma, L. *Int. Journal of Hydrogen Energy* **2009**, *34*, 4788.

(3) Johnson, A. D.; Daley, S. P.; Utz, A. L.; Ceyer, S. T. *Science* **1992**, *207*, 223.

(4) Maynard, K.; Daley, S.; Yang, Q.; Ceyer, S. *Phys.Rev.Lett.* **1991**, *67*, 927.

(5) Song, J.; Curtin, W. A. *Nature* **2013**, *12*, 145.

(6) Bockris, J. O.; Khan, S. *Surface Electrochemistry: A Molecular Level Approach*; Plenum Press, 1993; Vol. 3.

(7) Gennero, M.; Chialvo, A. *J. Electroanal. Chem.* **1994**, *372*, 209.

(8) Quaino, P.; Gennero, M.; Chialvo, A. *Electrochim. Acta* **2007**, *52*, 7396.

(9) Bagotskaya, I. *Zh. Fiz. Khim* **1962**, *36*, 2667.

(10) Frumkin, A. *Advances in Electrochemistry and Electrochemical Engineering*; Interscience Pub., 1963; Vol. 3.

(11) Bockris, J. O.; McBreena, J.; Nanis, L. *J. Electroanal. Chem.* **1965**, *112*, 1025.

(12) Sakong, S.; Mosch, C.; Lozano, A.; Busnengo, H.; Gross, A. *ChemPhysChem* **2012**, *13*, 3467.

(13) Jerkiewicz, G. *Prog. Surf. Sci.* **1998**, *57*, 137.

(14) Hu, C. C.; Wen, T. C. *J. Electrochem. Soc.* **1995**, *142*, 1376.

(15) Christmann, K. *Hydrogen Adsorption on Metal Surfaces*; Plenum Press, NY, 1983; Vol. 5.

(16) Roudgar, A.; Gross, A. *Phys. Rev. B* **2003**, *67*, 033409.

(17) Roudgar, A.; Gross, A. *J. Electroanal. Chem.* **2003**, *548*, 121.

(18) Gross, A. *Top. Catal.* **2006**, *37*, 29.

(19) Venkatachalam, S.; Jacob, T. *Phys. Chem. Chem. Phys.* **2009**, *11*, 3263.

(20) Björketun, M.; Karlsberg, G.; Rossmeisl, J.; Chorkendorff, I.; Wolfschmidt, H.; Stimming, U.; Nørskov, J. *Phys. Rev. B* **2011**, *84*, 045407.

(21) Mavrikakis, M.; Hammer, B.; Nørskov, J. *Phys. Rev. Lett.* **1998**, *81*, 2819.

(22) Ruban, A.; Hammer, B.; Stoltze, P.; Skriver, H.; Nørskov, J. *J. Mol. Catal. A: Chem.* **1997**, *115*, 421.

(23) Santos, E.; Quaino, P.; Schmickler, W. *Electrochim. Acta* **2010**, *55*, 4346.

(24) Quaino, P.; Santos, E.; Wolfschmidt, H.; Montero, M.; Stimming, U. *Catal. Today* **2011**, *177*, 53.

(25) Santos, E.; Hindelang, P.; Quaino, P.; Schulz, E.; Soldano, G.; Schmickler, W. *ChemPhysChem* **2011**, *12*, 2274.

(26) Soldano, G.; Quaino, P.; Santos, E.; Schmickler, W. *ChemPhysChem* **2010**, *11*, 2361.

(27) Santos, E.; Quaino, P.; Soldano, G.; Santos, E.; Schmickler, W. *Electrochem. Comm.* **2009**, *11*, 1764.

(28) Lovvik, O.; Olsen, R. *Phys.Rev.B* **1998**, *58*, 10890.

(29) Paul, J.; Sautet, P. *Phys. Rev.B* **1996**, *53*, 8015.

(30) Greeley, J.; Mavrikakis, M. *Surface Science* **2003**, *540*, 215.

(31) Jiang, D.; Carter, E. *Phys.Rev.B* **2004**, *70*, 64102.

(32) Peden, J. Y. J. C.; Houston, J.; Goodman, D. *Surface Science* **1985**, *160*, 37.

(33) Hennig, D.; Wilke, S.; Löber, R.; Methfessel, M. *Surface Science* **1993**, *287-288*, 89.

(34) Löber, R.; Henning, D. *Phys. Rev. B* **1997**, *55*, 4761.

(35) Yu, W.; Mullen, G. M.; Mullins, C. B. *J. Phys. Chem. C* **2013**, *117*, 19535.

(36) Ogura, S.; Okada, M.; Fukutani, K. *J. Phys. Chem. C* **2013**, *117*, 9366.

(37) Quaino, P.; Santos, E. *Langmuir* **2015**, *31*, 858.

(38) Juárez, M. F.; Soldano, G.; Guesmi, H.; Tielens, F.; Santos, E. *Surface Science* **2015**, *631*, 235.

(39) Hammer, B.; Hansen, L. B.; Nørskov, J. K. *Phys. Rev. Lett.* **1996**, *59*, 7413.

(40) Vanderbilt, D. *Phys. Rev. B* **1990**, *41*, 7892.

(41) Monkhorst, H. J.; Pack, J. D. *Phys. Rev. B* **1976**, *76*, 5188.

(42) Perdew, J. P.; Burke, K.; Ernzerhof, M. *Phys. Rev. Lett.* **1996**, *77*, 3865.

(43) Kittel, C. *Introducción a la física del estado sólido*; Edición en español, Editorial Reverté, S.A., 1975-1976.

(44) Perdew, J. P.; Chevary, J. A.; Vosko, S. H.; Jackson, K. A.; Pederson, M. R.; Singh, D. J.; ; Fiolhais, C. *Phys. Rev. B* **1992**, *46*, 6671.

(45) Bengtsson, L. *Phys. Rev. B* **1999**, *59*, 12301.

(46) Henkelman, G.; Uberuag, B. P.; Jonsson, H. *J. Chem. Phys.* **2000**, *113*, 9901.

(47) Henkelman, G.; Jonsson, H. *J. Chem. Phys.* **2000**, *113*, 9978.

(48) Zhdanov, V. *Elementary Physicochemical Processes on Solid Surfaces*; Springer, 1991.

(49) Nazmutdinov, R.; Bronshtein, M.; Wilhelm, F.; Kuznetsov, A. *J. Electroanal. Chem.* **2007**, *607*, 175.

(50) Gross, A. *Adsorption at nanostructured surfaces in Handbook of Theoretical and Computational Nanotechnology*; American Scientific Publishers, 2006; Chapter 89.

(51) Baldauf, M.; Kolb, D. *Electrochim. Acta* **1993**, *38*, 2145.

(52) Meier, J.; Schiotz, J.; Liu, P.; Nørskov, J.; Stimming, U. *Chem. Phys. Lett* **2004**, *390*, 440.

(53) Meier, J.; Friedrich, K.; Stimming, U. *Faraday Discuss* **2002**, *121*, 365.

(54) Wolfschmidt, H.; Weingarth, D.; Stimming, U. *ChemPhysChem* **2010**, *11*, 1533.

(55) Hammer, B.; Nørskov, J. *Surface Science* **1995**, *343*, 211.

(56) Ruban, A.; Hammer, B.; Stoltze, P.; Skriver, H.; Nørskov, J. *J. Mol. Catal. A: Chem.* **1997**, *115*, 421.

(57) Roudgar, A.; Gross, A. *Surface Science* **2005**, *597*, 42.

(58) Dong, W.; Ledentu, V.; Sautet, P.; Eichler, A.; Hafner, J. *Surface Science* **1998**, *411*, 123.

(59) Lischka, M.; Gross, A. *Recent Developments in Vacuum Science and Technology*; Research Signpost, Kerala, India, 2003; Chapter Hydrogen on palladium: a model system for the interaction of atoms and molecules with metal surfaces.

(60) M.Baldauf,; Kolb, D. *Electrochim. Acta* **1993**, *38*, 2145.

(61) Santos, E.; Lundin, A.; Pötting, K.; Quaino, P.; Schmickler, W. *Physical Review B* **2009**, *79*, 235436.

(62) Calleja, F.; García-Suárez, V.; Hinarejos, J.; J. Ferrer, A. V. d. P.; Miranda, R. *Phys. Rev. B* **2005**, *71*, 125412.

(63) Duncan, H.; Lasia, A. *Electrochim. Acta* **2008**, *53*, 6845.

(64) Loeber, R.; Hennig, D. *Phys. Rev.* **1997**, *55*, 4761.

(65) Ozawa, N.; Arboleda, N.; Roman, T.; Nakanishi, H.; Dino, W.; Kasai, H. *J. Phys.: Condens. Matter* **2007**, *19*, 365214.

(66) Olsen, R.; Philipsen, P.; Baerend, E.; Kroes, G. J.; Løvvik, O. M. *J. Chem. Phys.* **1997**, *106*, 9286.

(67) Olsen, R. A.; Kroes, G. J.; Løvvik, O. M.; Baerends, E. J. *J. Chem. Phys.* **1997**, *107*, 10652.

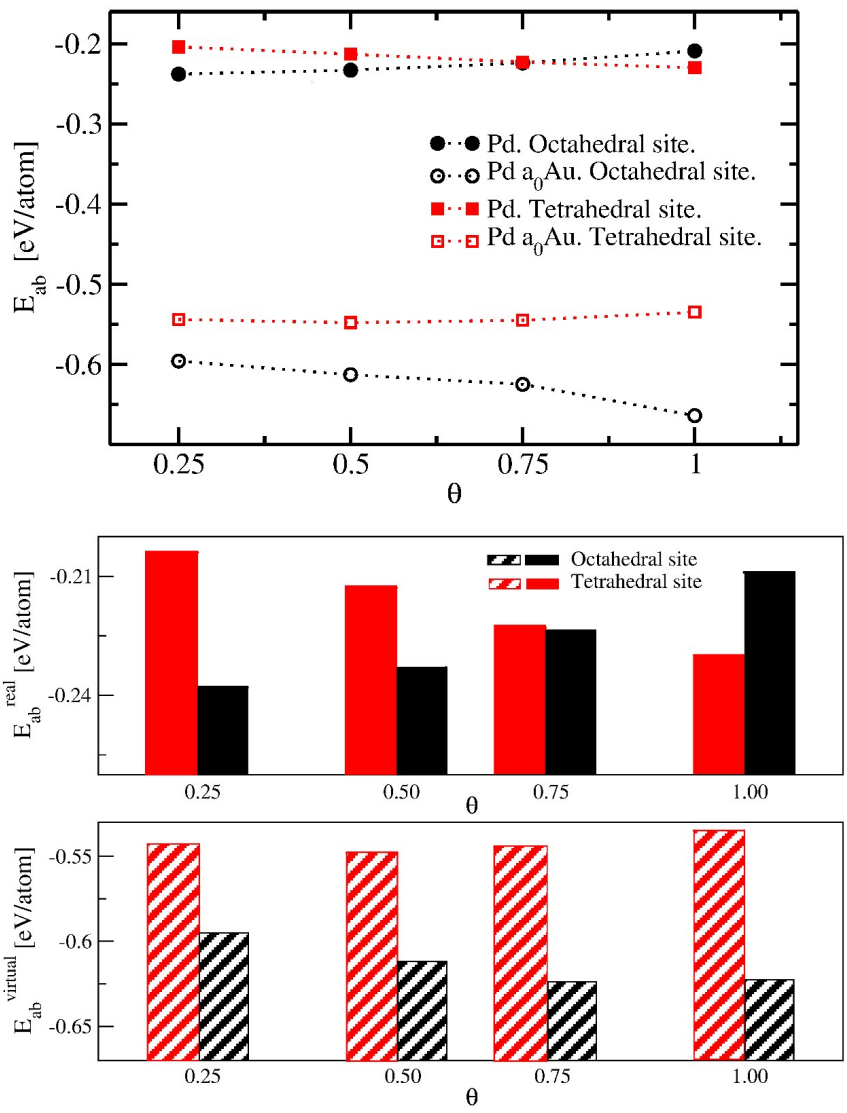

Figure 7: Absorption energies in eV/atom as a function of the hydrogen concentration for Pd(111) with a_0^{Au} and Pd(111). Octahedral (black dotted line) and tetrahedral (red dotted line) sites were considered. Bar plots are also added for better interpretation – middle graph: real system, bottom graph: virtual system.

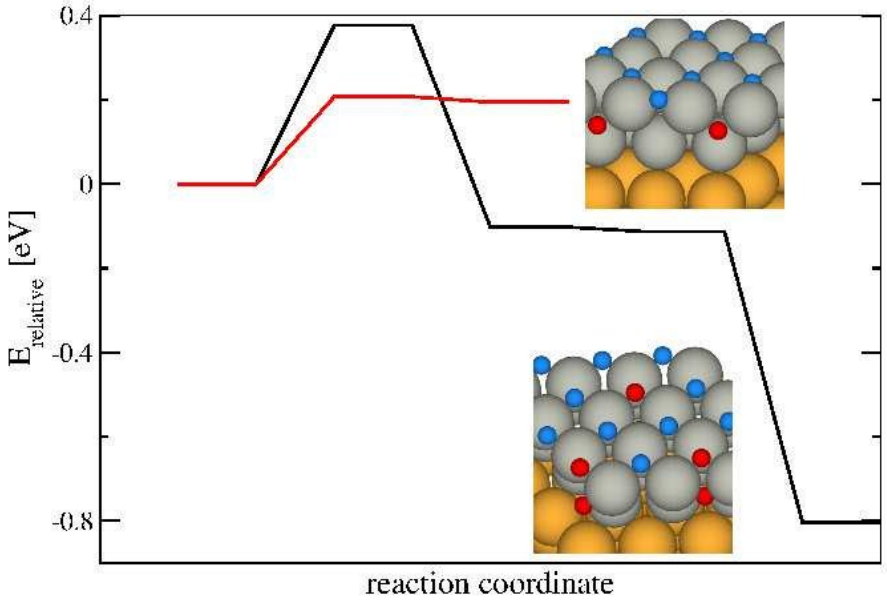

Figure 8: Red line:Reaction scheme for the hydrogen subsurface penetration from a monolayer of pre-adsorbed hydrogen or the well known H_{UPD}. Black line: Reaction scheme for the hydrogen subsurface penetration upon H_2 adsorption and bond breaking. Final states are shown for each case. Different type of atoms are represented in specific colors: H (light blue), Pd(grey) and Au(yellow). The initial configuration is used as reference to calculate the energy difference. Structure details for each path are shown in the ESI